Supporting Information

Fe-Assisted Nitridation-Induced Reconstruction of Mo-Fe-Ni Molybdates Enables Durable Alkaline Seawater Oxygen Evolution and Zn-Air Batteries

Hamza M. Haruna,[a,b] Yanxiang He,[a] Zhixiao Zhu,[a] Hao Yang,[c] Selvam Mathi[a,*] Guanhua Zhang,[b,*] Zhongmin Wang,[d] and M.-Sadeeq Balogun[a,d,*]

[a]College of Materials Science and Engineering, Hunan Joint International Laboratory of Advanced Materials and Technology for Clean Energy, Hunan University, Changsha, 410082, People's Republic of China.

[b]College of Mechanical and Vehicle Engineering, Hunan University, Changsha 410082, P. R. China

[c]School of Chemistry & Chemical Engineering, Guangxi Key Laboratory of Electrochemical Energy Materials, Guangxi Colleges and Universities Key Laboratory of Applied Chemistry Technology and Resource Development. Guangxi University, Nanning, 530004, China

[d]Guangxi Academy of Sciences, Nanning, Guangxi, 530007, People's Republic of China.

*Corresponding Authors E-mail:

ssmathi09@hnu.edu.cn (S. Mathi)

balogun@hnu.edu.cn (M.-Sadeeq Balogun)

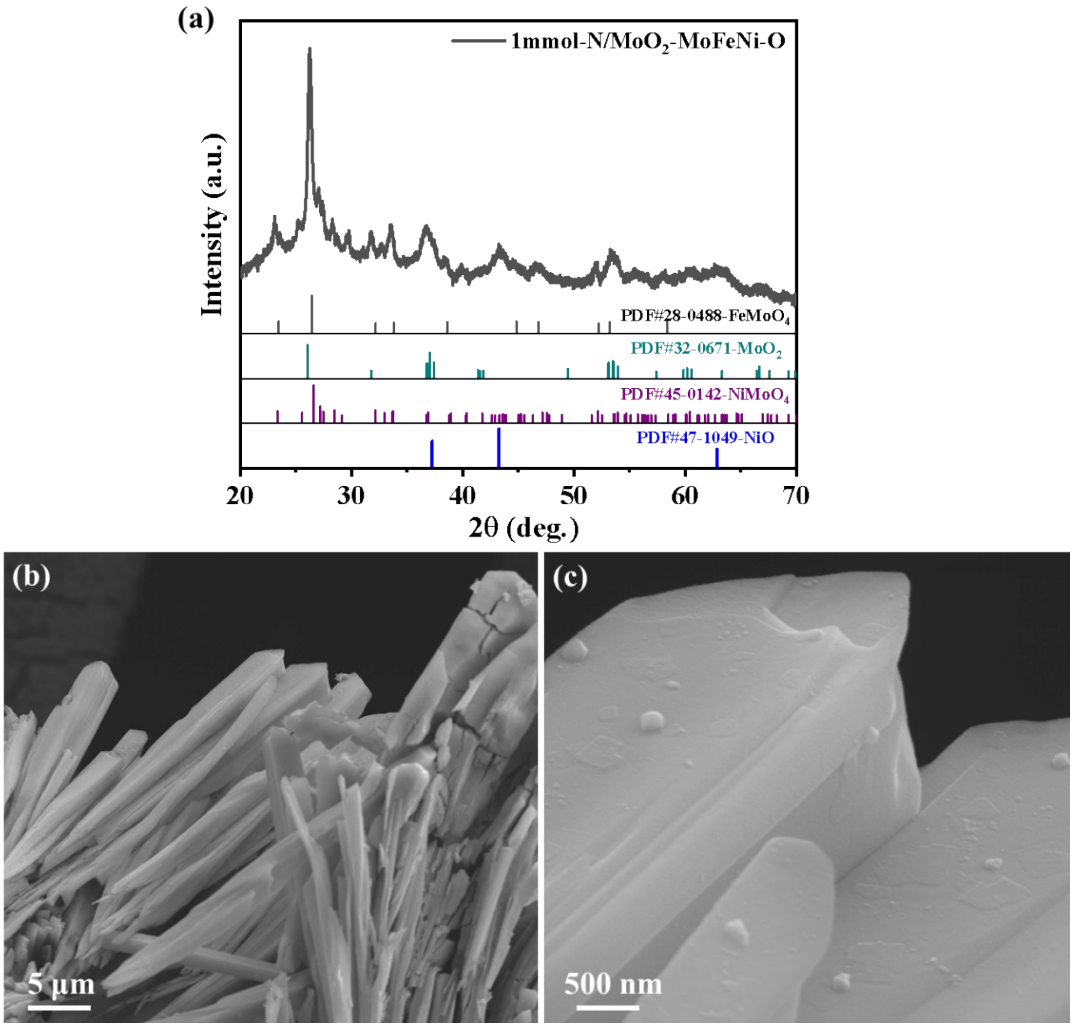

Figure S1. (a) XRD pattern, (b-c) SEM images of 1mmol-N/MoO_2-MoFeNi-O.

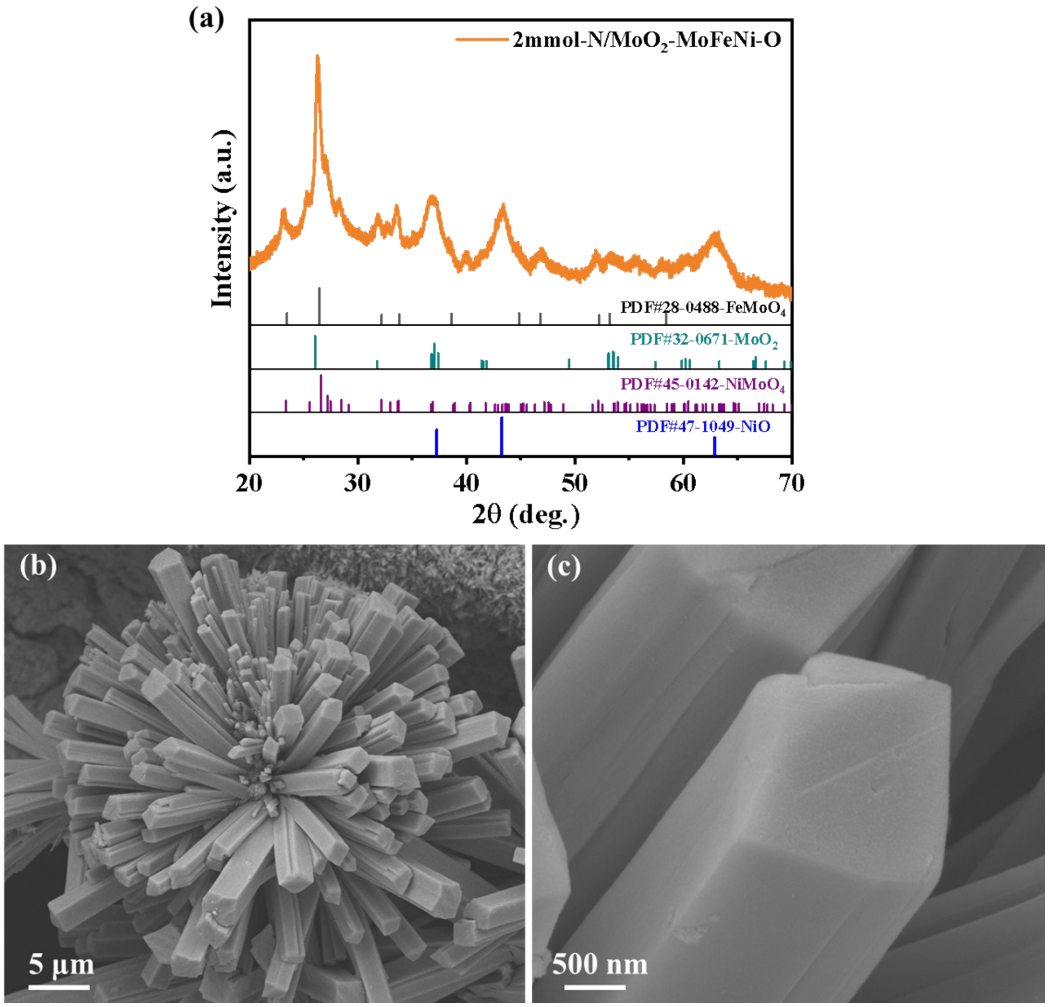

Figure S2. (a) XRD pattern, (b-c) SEM images of 2mmol-N/MoO_2-MoFeNi-O.

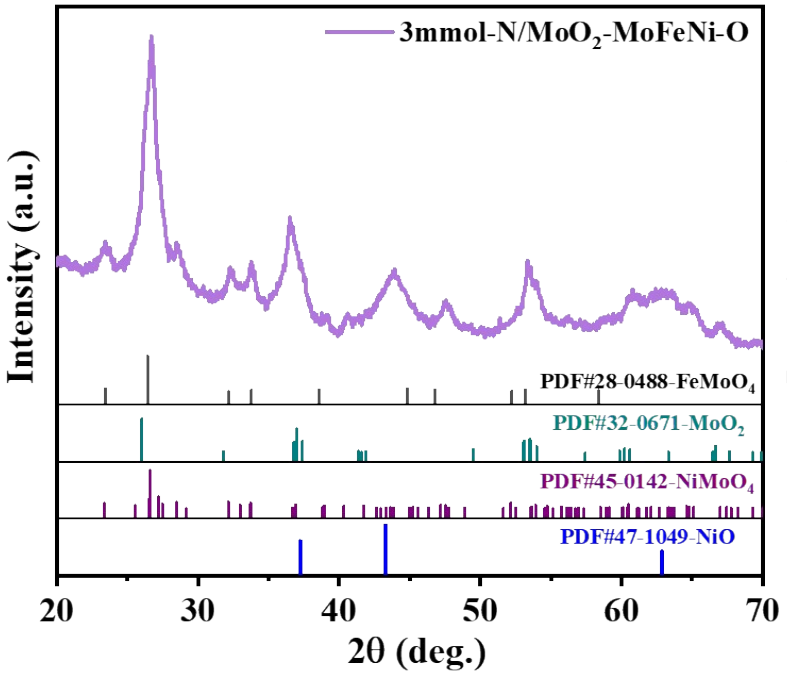

Figure S3. XRD pattern of 3mmol-N/MoO_2-MoFeNi-O.

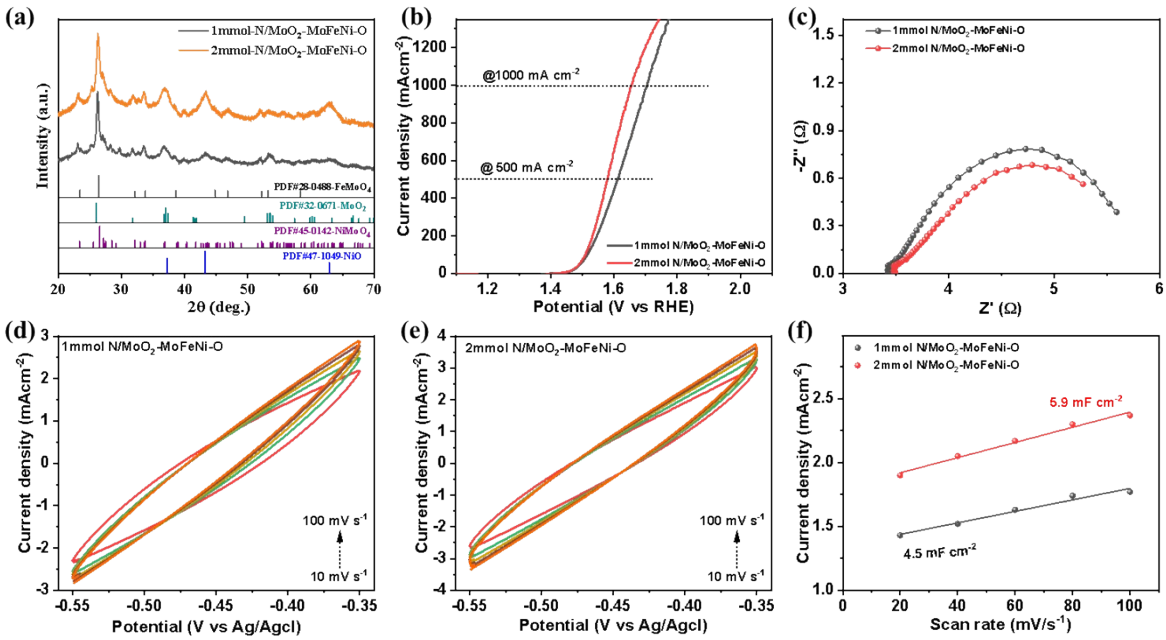

Figure S4. Structural and electrochemical analysis of 1mmol- and 2mmol-N/MoO_2-MoFeNi-O. (a) XRD patterns, (b) OER LSV curves, and (c) EIS spectra of 1mmol- and 2mmol-N/MoO_2-MoFeNi-O. CV curves of (d) mmol-N/MoO_2-MoFeNi-O and (e) 2mmol-N/MoO_2-MoFeNi-O. (f) ECSA comparison of 1mmol- and 2mmol-N/MoO_2-MoFeNi-O.

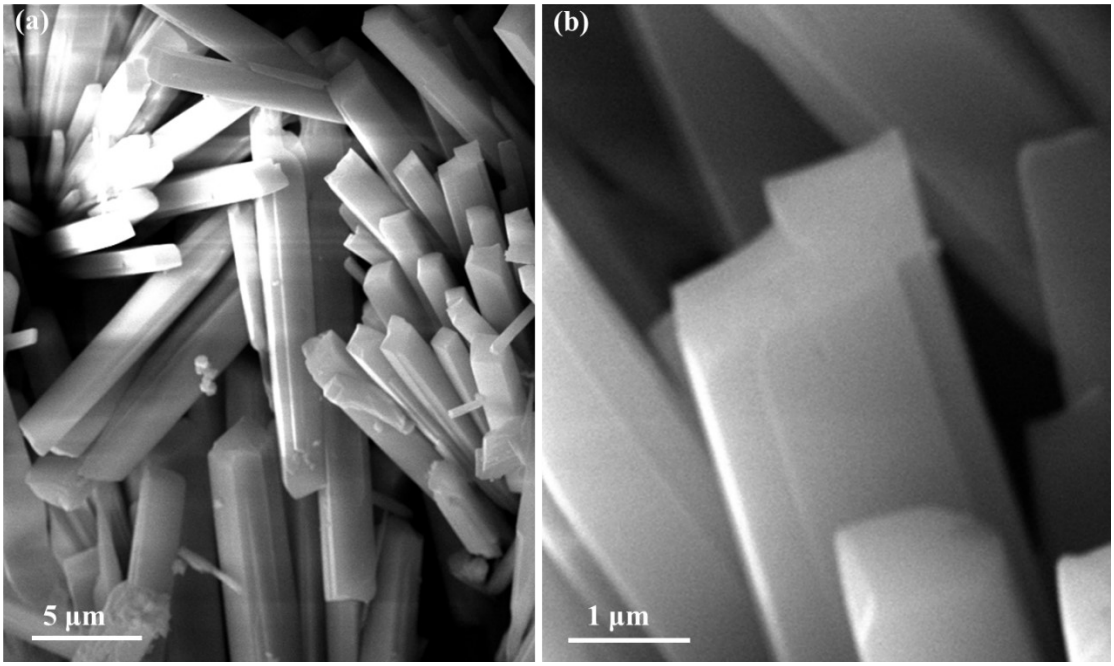

Figure S5. SEM images of the 4:3 (Fe:Mo) FeMo precursor.

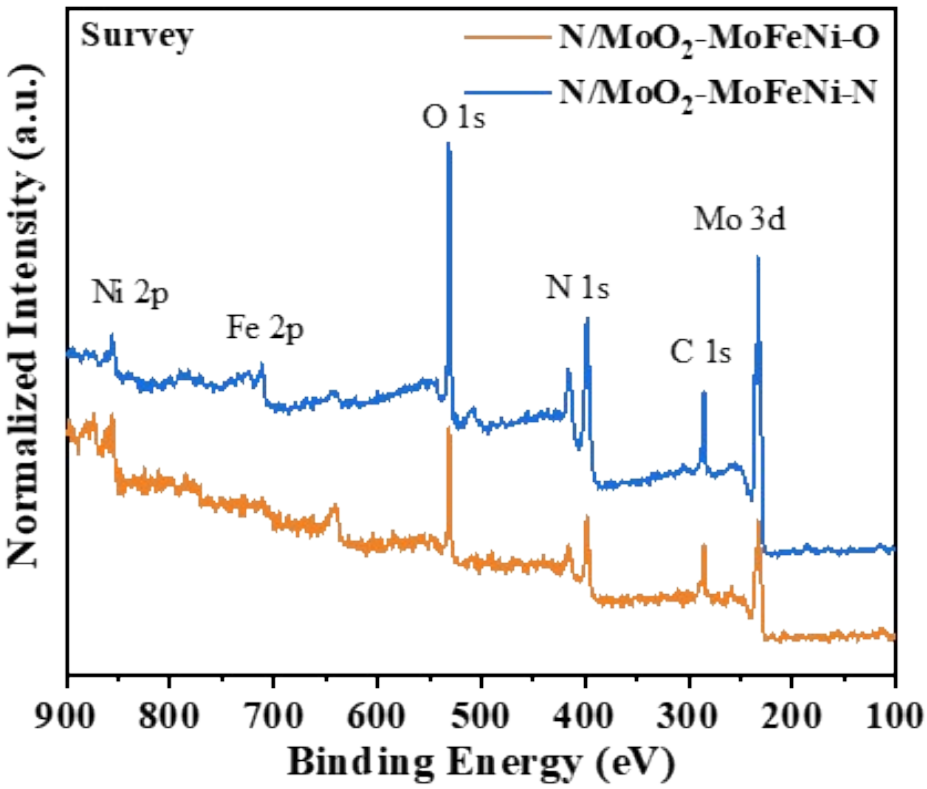

Figure S6. XPS survey spectra of N/MoO_2-MoFeNi-O and N/MoO_2-MoFeNi-N.

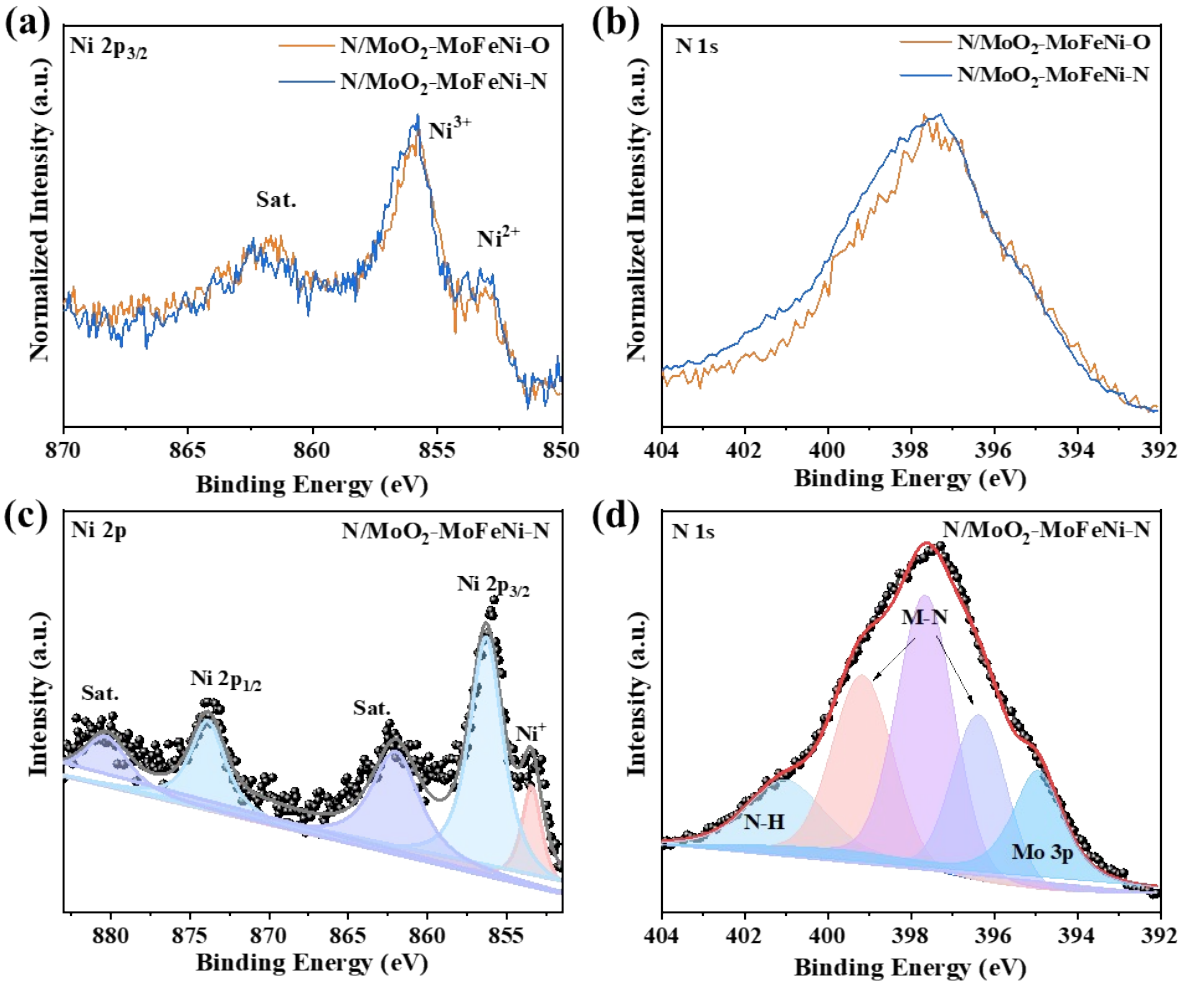

Figure S7. Normalized XPS spectra of (a) Ni 2p and (b) N 1s for N/MoO_2-MoFeNi-O and N/MoO_2-MoFeNi-N. Deconvoluted (c) Ni 2p and (d) N 1s XPS spectra of spectra of N/MoO_2-MoFeNi-N.

Table S1. Comparison of some recently reported representative transition metal-based electrocatalysts for OER in alkaline electrolytes.

Electrocatalysts	η10 (mV)	Tafel Slope ($mV\ dec^{-1}$)	Ref.
N/MoO_2-MoFeNi-N	**200**	**62**	**This work**
N/MoO_2-MoFeNi-O	220	65	This work
$Co_5Mo_{1.0}O$ NSs@NF	270	54.4	Nano Energy 45 (2018) 448-455.
Co_4Mo_2@NC	330	49	J. Mater. Chem. A 5 (2017) 16929-16935.
Fe_1Co_1-ONS	308	36.8	Adv. Mater. 29 (2017) 1606793.
PNG-$NiCo_2O_4$	349	156	ACS Nano 7 (2013) 10190-10196.
$CoFe_2O_4$	410	82	Nanoscale 7 (2015) 8920-8930.
$CoCr_2O_4$	422	63	Small 12 (2016) 2866-2871.
NiMnO NM	275	41	Electrochim. Acta 245 (2017) 32-40.
$MnFe_2O_4$	520	114	Nanoscale 7 (2015) 8920-8930.
$Co_6Mo_6C_2$/NCRGO	260	50	ACS Appl. Mater. Interfaces 2017, 9, 20, 16977-16985
Co_3Mo_3C/N-C	316	89.9	Int. J. Hydrogen. Energ. 46 (2021) 22268-e22276

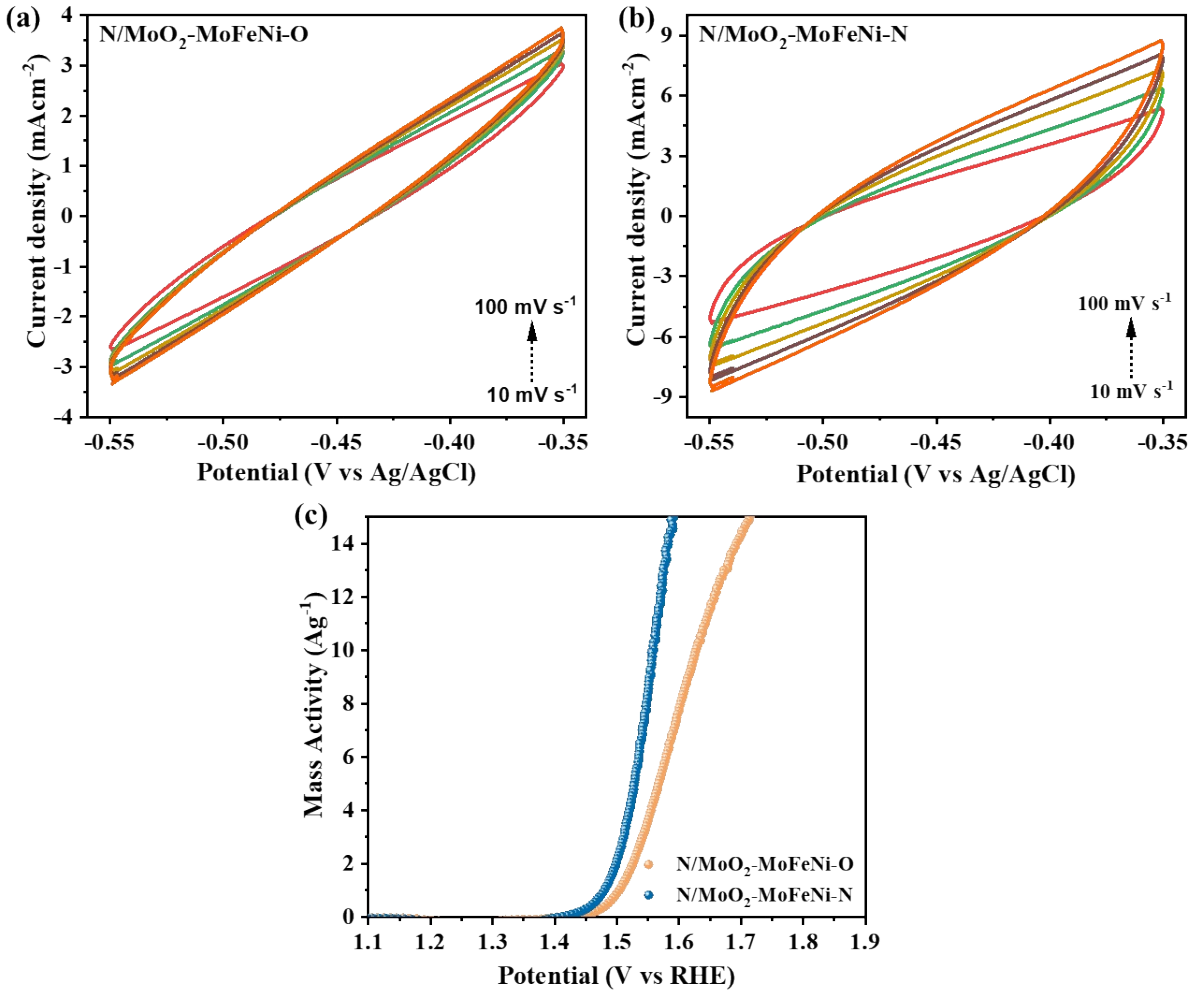

Figure S8. CV curves of (a) N/MoO_2-MoFeNi-O and (b) N/MoO_2-MoFeNi-N.

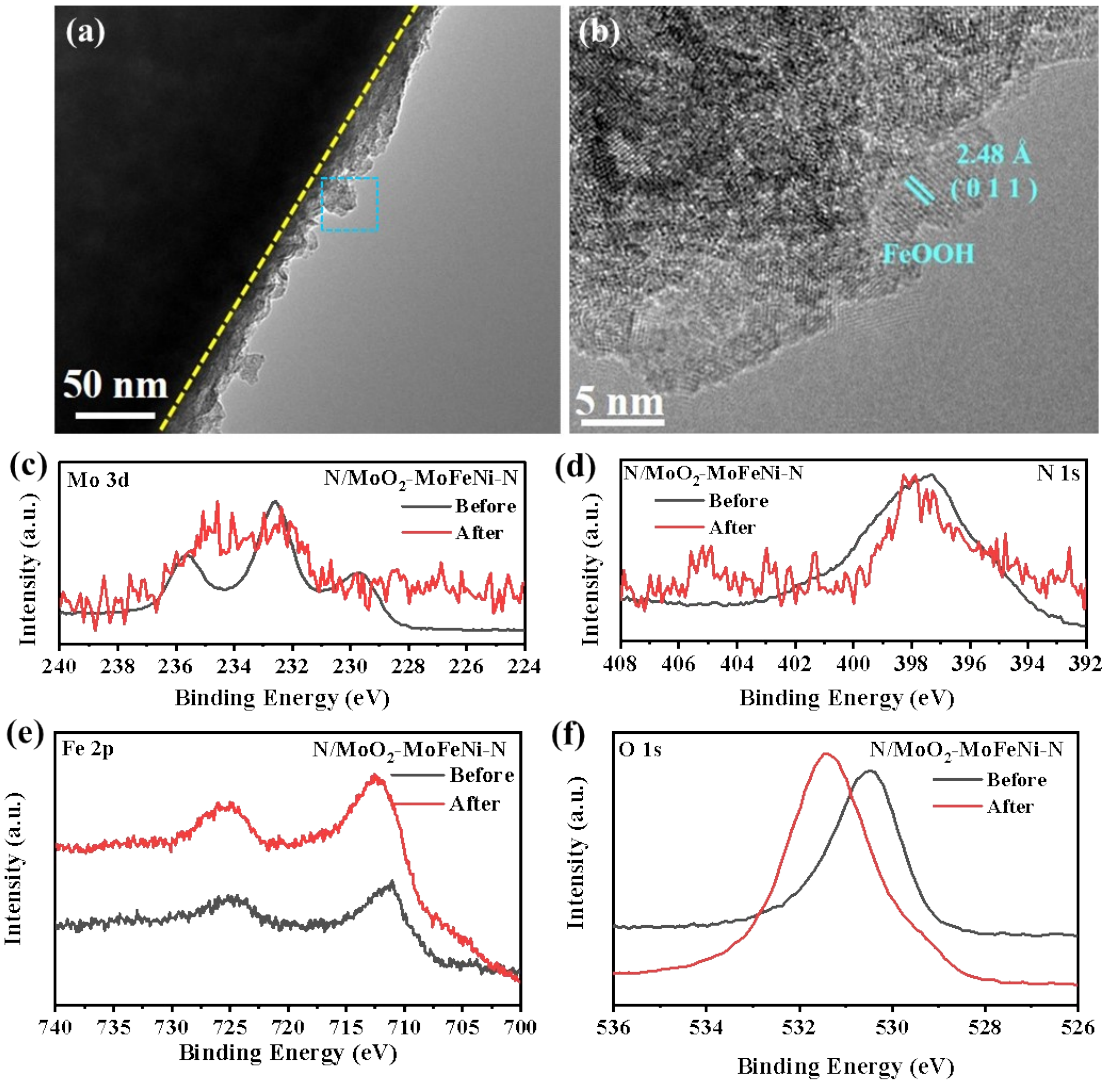

Figure S9. (a) TEM and (b) HRTEM images, and corresponding XPS spectra showing (c) Mo 3d, (d) N 1s, (e) Fe 2p, and (f) O 1s of N/MoO_2-MoFeNi-N after the stability test in freshwater KOH electrolyte.

Table S2. Comparison of OER performance of N/MoO_2-MoFeNi-N in freshwater and seawater electrolytes.

Electrolyte	η @ 500 mA cm^{-2}	η @ 1000 mA cm^{-2}	Tafel slope
Freshwater KOH	309 mV	392 mV	56.6 mV dec^{-1}
Seawater KOH	334 mV	499 mV	71.1 mV dec^{-1}

Table S3. Comparison of OER metrics in freshwater and seawater KOH electrolytes and with other reported literatures.

Electrocatalysts	Freshwater KOH η(mV) @500/1000mAcm^{-2}	Seawater KOH η(mV) @500/1000mAcm^{-2}	References
N/MoO_2-MoFeNi-N	**309/334**	**392/499**	**This work**
RuMoNi	390/480	397/484	Nat Commun 14, 3607 (2023).
Cr-Co_xP	NA	392/423	Adv. Funct. Mater. 2023, 33, 2214081
NixCryO	NA	460/-	Angew. Chem., Int. Ed. 2023, 62, e202309854
S-(Ni,Fe)OOH	NA	398/462	Energy Environ. Sci., 2020, 13, 3439-3446
Ni_3FeN@C/NF	341/-	394/-	J. Mater. Chem. A, 2021, 9, 13562
NiCoS/NF	330/390	440/470	Appl. Catal. B Environ., 2021, 291, 120071
NiFe-PBA-gel-cal /GC	398/-	NA	Adv. Sci. 2022, 9, 2200146
$MnCo_2O_4$@NiFe-LDH/NF	NA	578/-	J. Colloid Interface Sci. 2023, 632, 54
S-Cu_2O-CuO NDLs	400/450	440/-	Catal. Today 2022, 400-401, 14-25
NiCoHPi@Ni_3N/NF	405/-	474/-	ACS Appl. Mater. Interfaces 2022, 14, 22061-22070
FeCoNiCrMn HEA/NM	-/330	NA	J. Mater. Chem. A, 2025,13, 17384-17392

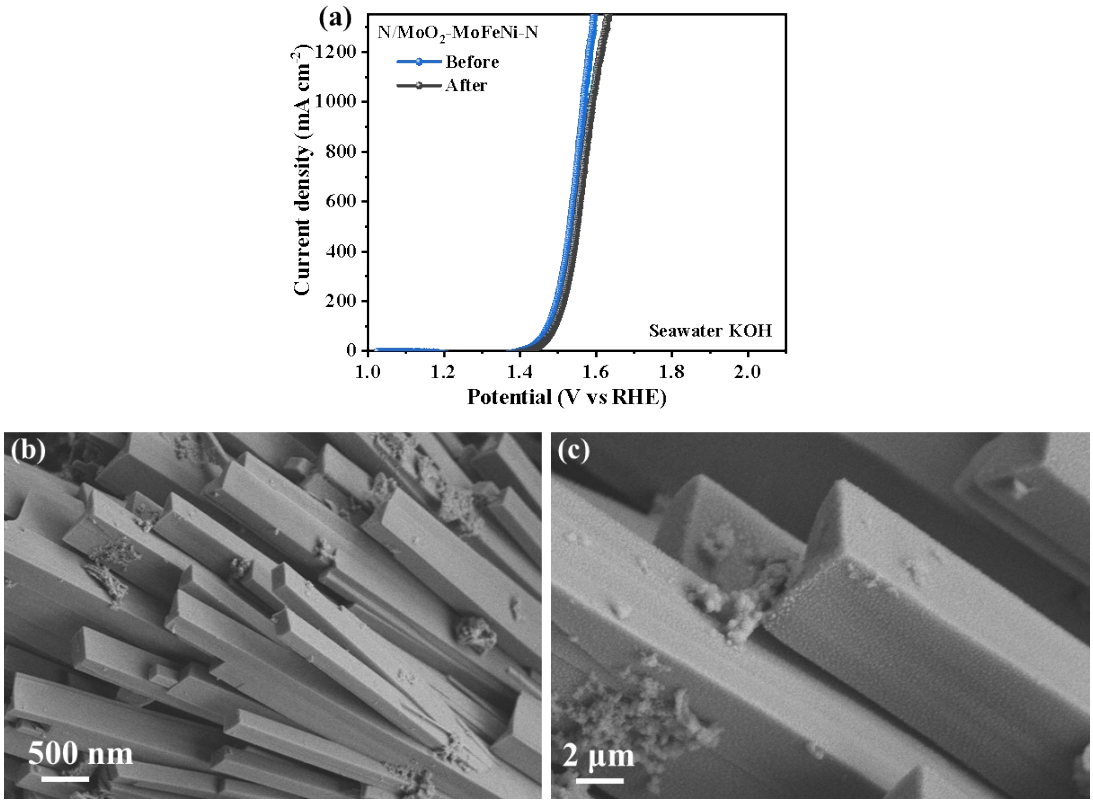

Figure S10. (a) LSV curves before and after seawater stability test and (b-c) SEM images of N/MoO_2-MoFeNi-N after the stability test.

Figure S11. Digital image of pH-adjusted 6 M KOH seawater electrolyte after DPD addition.

Table S4. ICP analysis of electrolyte before and after electrolysis in alkaline seawater

Element	Before electrolysis (mg L^{-1})	After electrolysis (mg L^{-1})
Mo	0.0	0.0
Fe	0.0	1942.2
Ni	192.0	12446.5

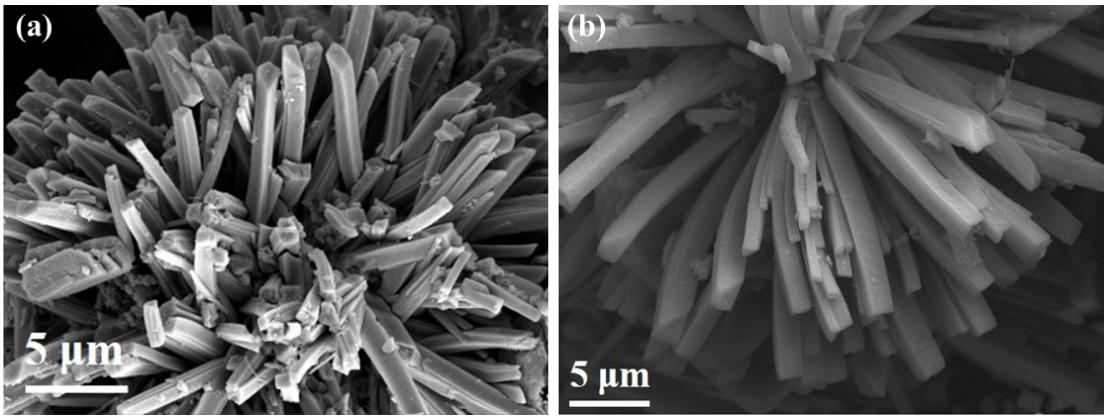

Figure S12. SEM images of N/MoO_2-MoFeNi-N after the OWS stability test in (a) alkaline freshwater and (b) alkaline seawater.

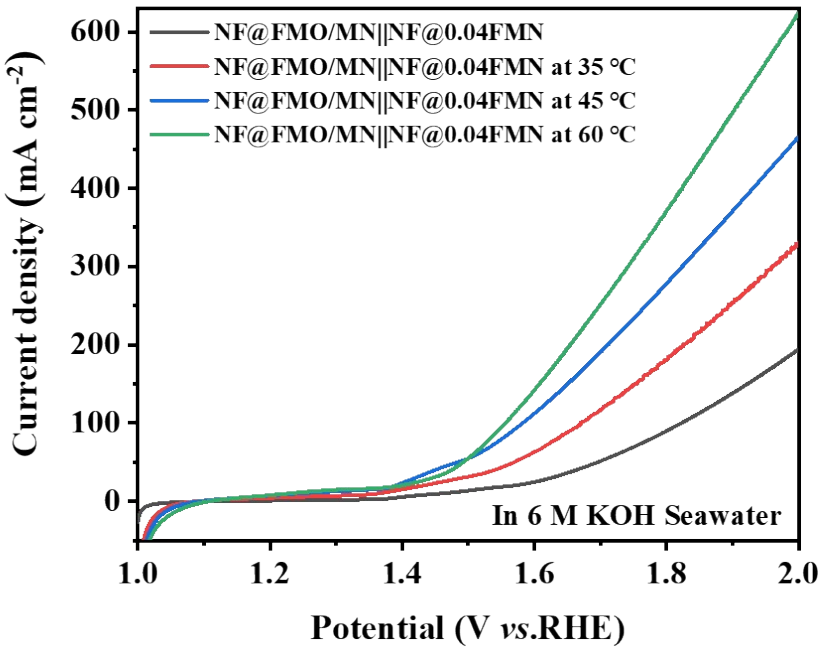

Figure S13. OWS LSV curves at different temperatures in 6 M KOH.

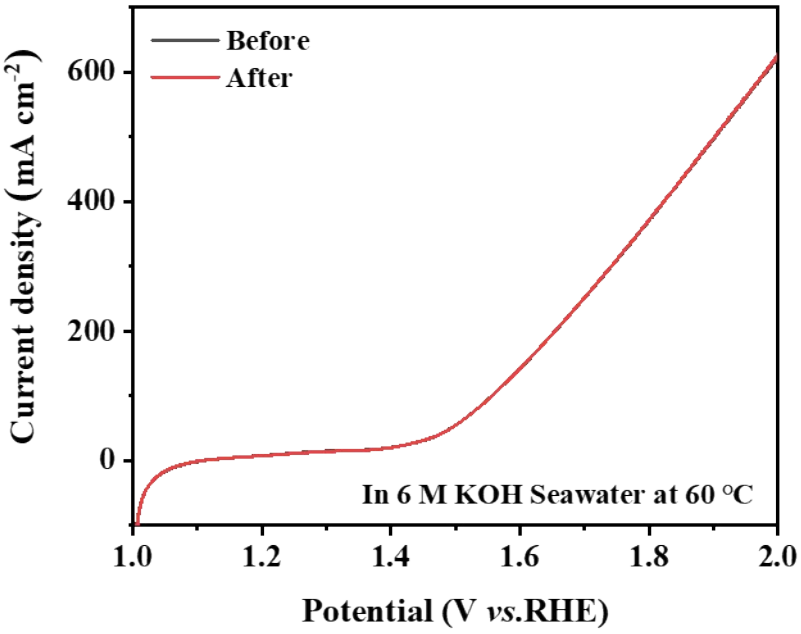

Figure S14. (a) LSV curves of N/MoO_2-MoFeNi-N before and after seawater stability test in 6.0 M seawater KOH electrolyte over 60 °C.

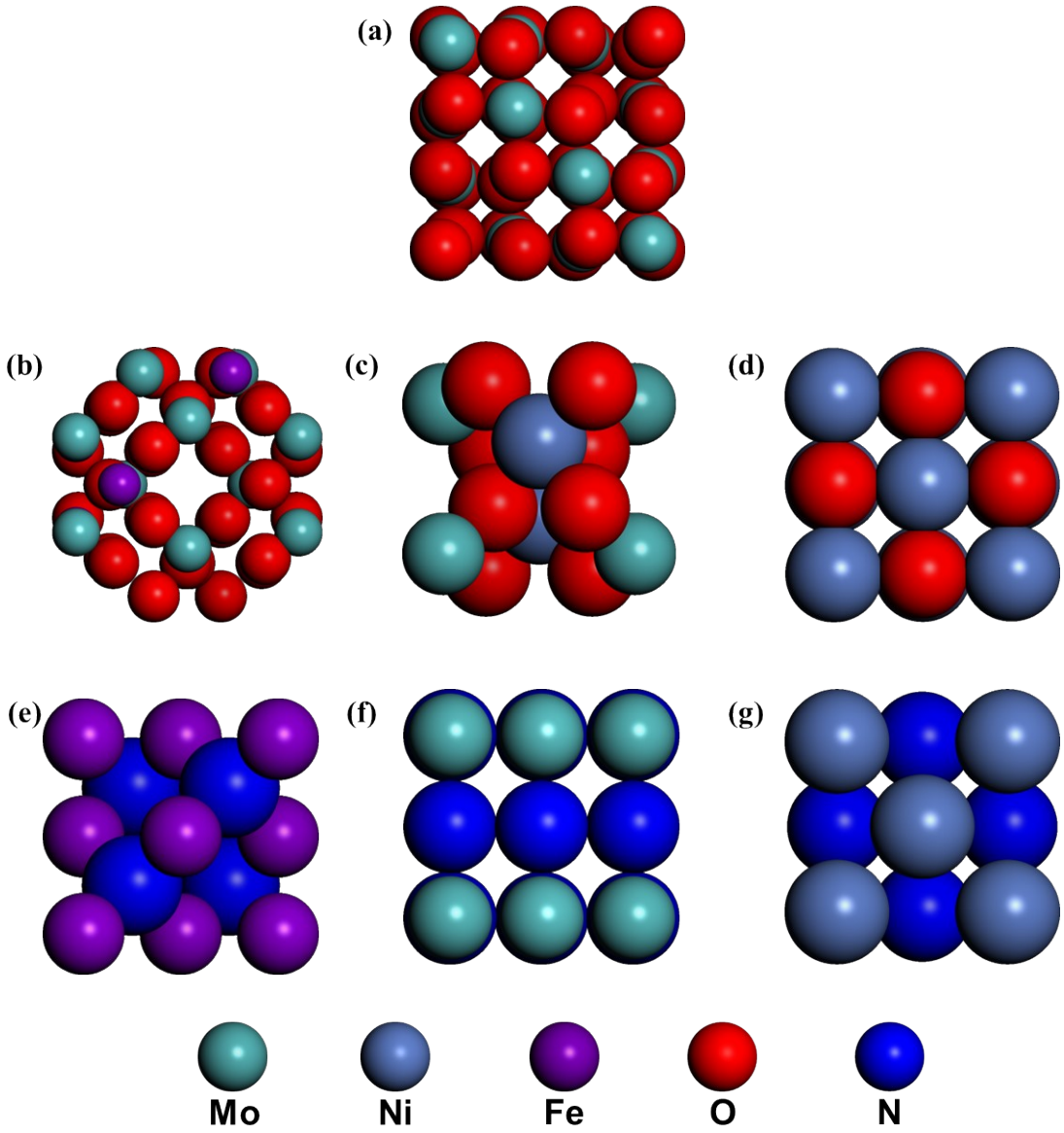

Figure S15. Optimized structural models of (a) MoO_2, (b) $FeMoO_4$, (c) $NiMoO_4$, (d) NiO, (e) FeN, (f) Mo_2N, and (g) Ni_4N.

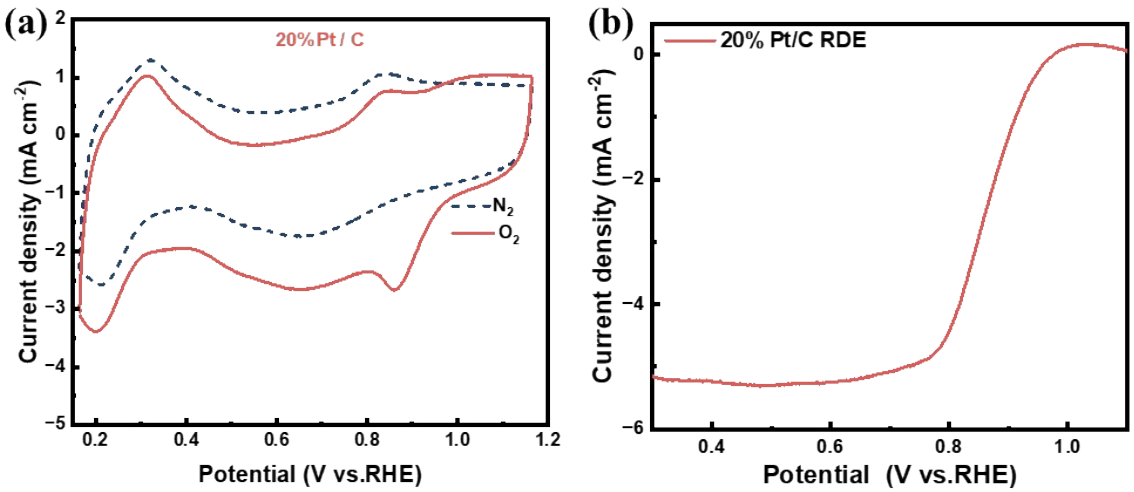

Figure S16. (a) CV curves recorded in 0.1 M KOH saturated with O_2 (solid lines) and N_2 (dotted lines) at a scan rate of 50 mV s^{-1} and (b) ORR LSV curves at rotation speeds of 1600 rpm of the Pt/C electrocatalyst.

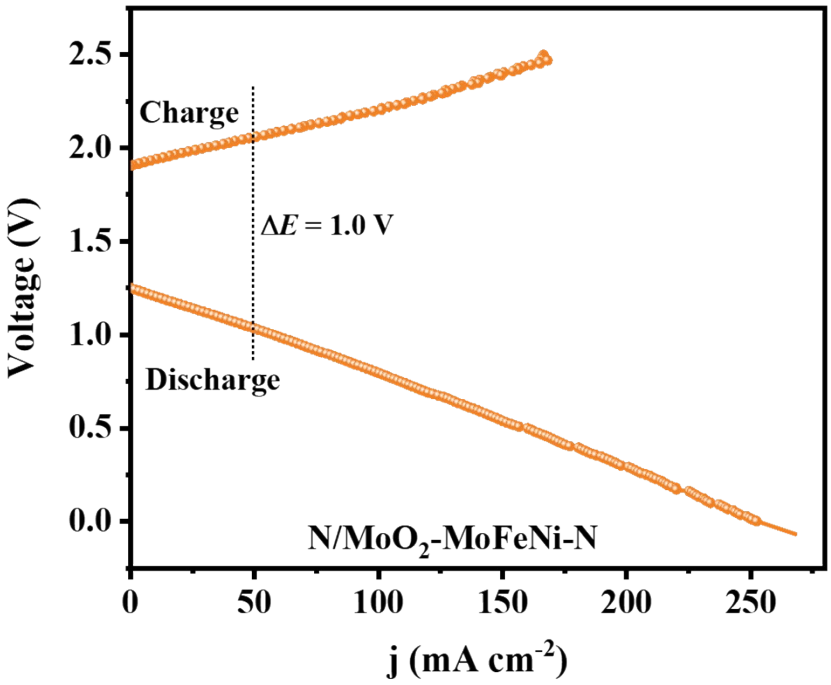

Figure S17. ORR charging and discharging I-V polarization curves of N/MoO_2-MoFeNi-N.

Table S5. Comparison of the as-prepared N/MoO_2-MoFeNi-N with reported ORR catalysts.

Electrocatalysts	Peak power density ($mW\ cm^{-2}$)	Cycling stability (h)	References
N/MoO_2-MoFeNi-N	**84.2 mW cm^{-2}**	**140 @10mA cm^{-2}**	**This work**
$Cu_{0.81}Ni_{0.19}$@CoN/Mo_2N	81.72	150@10mA cm^{-2}	Chem. Eng. J., 2026, 528, 172033
NS@$Co_{3-x}Ni_xO_4$/Co_3O_4	-	200 @5mA cm^{-2}	Energy Stor. Mater., 24 (2020) 272-280
$MnCo_2O_{4.5}$NPs	-	6 @10mA cm^{-2}	J. Appl. Electrochem., 50 (2020) 907-915
Co_3O_4 nanowire	35.7	333@10mA cm^{-2}	Appl. Catal. B., 241 (2019) 104-112
GCCCO	81.6	20@5mA cm^{-2}	Appl. Catal. B, 358 (2024) 124354
2%Cu-Co_3O_4	-	100@5mA cm^{-2}	ACS Appl. Mater. Interfaces, 16 (2024) 17574
L8S2MCO/Vulcan	44.5	20@5mA cm^{-2}	J. Power Sources, 632 (2025) 236364
VSM0.5CO	38.4	20@5mA cm^{-2}	Appl. Surf. Sci. Adv., 27 (2025) 100725
Co_9S_8/$Co_{1-x}S$/WS_2	52.2	100@10mA cm^{-2}	Electrochim. Acta, 512 (2025) 145467
5%Cu-Co_3O_4	84.4	140@5mA cm^{-2}	ACS Appl. Mater. Interfaces, 16 (2024) 17574
10%Cu-Co_3O_4	-	80@5mA cm^{-2}	ACS Appl. Mater. Interfaces, 16 (2024) 17574
$CoNi_2S_4$@CoNi-LDH	62.2	320@5mA cm^{-2}	J. Mater. Chem. C, 11 (2023) 16384-16389